Challenges and Opportunities for the Mechanical Reliability of Metal-Halide Perovskites and Photovoltaics

Zhenghong Dai and Nitin P. Padture*

School of Engineering, Brown University, Providence, RI 02912, USA

* *Email: nitin_padture@brown.edu*

Invited Perspective Article, *Nature Energy*, in press (2023)

The unproven reliability of perovskite photovoltaics (PV) is likely to pose a significant technical hurdle in the path towards the widespread deployment of the technology. The overall reliability of perovskite PV is directly affected by the mechanical reliabilities of the metal-halide perovskite materials, cells, and modules, but this issue has been largely overlooked. Here we stress the importance of addressing the mechanical reliability issue comprehensively. We highlight the important challenges and opportunities, together with best practices, pertaining to the three key interrelated elements that determine the mechanical reliability of perovskite PV: driving stresses, mechanical properties, and mechanical failure. We discuss how to measure the driving stresses and the mechanical properties accurately, together with their evolution over time, and of the need for understanding the relevant failure mechanisms and coupled effects. This effort will inform scientific approaches for making perovskite PV more durable and help them reach their full potential.

Single-junction and tandem (with Si) perovskite PV for potential utility and rooftop applications have achieved high efficiencies.[1-3] Perovskite PV also offer other functionalities for possible uses as light-weight, flexible power sources for consumer applications;[4] building integration;[5] and space applications.[6] However, the intrinsic stability of metal-halide perovskite light-absorbers at the heart of perovskite PV remains an important challenge.[7] The overall reliability of perovskite PV is also influenced by in-service chemical degradation of materials induced by heat, environment, light, and electric-field, as well as adverse reactions between the functional layers within the PV.[8,9]

Mechanical reliability has direct bearing on the overall PV reliability, but it has been largely overlooked.[8,10,11] The issue of mechanical reliability is particularly critical in the case of perovskite PV because halide perovskites possess an unusual combination of poor mechanical properties, making them inherently more fragile than other PV materials.[12,13] To put this in perspective, the basic mechanical properties of the prototypical halide perovskite methylammonium lead triiodide ($CH_3NH_3PbI_3$ or $MAPbI_3$) are:[13] Young's modulus stiffness (E) of 10.6 GPa, hardness (H) of 0.76 GPa, fracture toughness (K_{IC}) of 0.18 MPa.m$^{0.5}$, and fracture energy ($G_C=K_{IC}^2/E$) of ~3.0 J.m^{-2}. These values are for single-crystals and represent upper bounds.[13] By comparison, the corresponding average properties of single-crystal Si are E~160 GPa,[14] H~14 GPa,[15] K_{IC}~1 MPa.m$^{0.5}$,[16] and G_C~6 J.m^2.

Perovskite PV are subjected to significant mechanical stresses (σ), and derived stress-intensity factor (K) or strain-energy release rate (G), that drive failure.[11,17,18] In this context, a strong connection between the operational stability of perovskite PV and their mechanical reliability was recently demonstrated,[19,20] although such correlations were implied previously.[12,17,21,22] Since perovskite PV are expected to retain their mechanical integrity not only

during operation, but also in manufacturing, installation and maintenance, mechanical reliability is an important technical hurdle that must be overcome before the technology can be commercialized successfully.

Box 1| Mechanical reliability concepts and analyses

The vast majority of purported mechanical-reliability research in the literature on halide perovskites and PV actually pertains to mechanical behavior in general. Mechanical reliability *per se* is described by failure probability, $P_F = x/(X+1)$, as a function of failure quantity (F_F), such as failure stress (σ_F), time to failure (t_F), cycles to failure (n_F), *etc*.; x is failure rank and X is number of tests. This is typically analyzed using Weibull distribution:[37]

$$P_F = 1 - \exp\left\{-\frac{V}{V_O}\left(\frac{F_F}{F_O}\right)^m\right\},$$

where m is the Weibull modulus, V is the volume of the tested material, V_O is the reference volume, and F_O is the corresponding reference failure quantity; larger m implies greater reliability.

Graphically, mechanical reliability of materials or/and devices can be simplistically thought of as competition between driving stresses (σ), or derived stress-intensity factor (K) or strain-energy release rate (G) ('offense'), and mechanical properties ('defense'), both of which may evolve over time (or cycles). Generally, the mechanical properties degrade over time/cycles, whereas the driving stresses may accumulate (buildup) or decay (relaxation) depending on the particular situation. Critical condition for mechanical failure is when they become equal, where the process is stochastic. The failure statistics are then analyzed using the above Weibull distribution.

Note that the terms reliability and durability are used somewhat interchangeably in the literature, but there is a difference. In the context of PV, reliability generally entails statistical measurement and analysis of failure of materials and devices as defined by certain criteria. In contrast, durability typically pertains to the modes and mechanisms by which materials and devices degrade and fail.

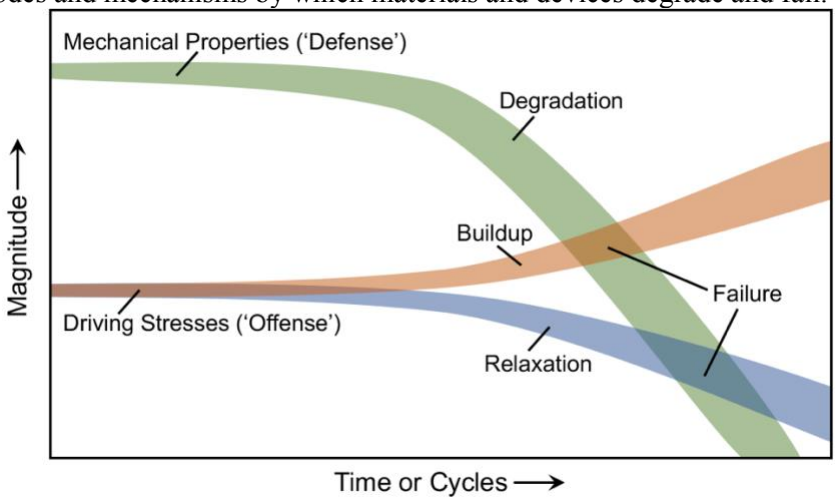

For meaningful analyses of mechanical reliability (Box 1), with the prospect of predicting material/device lifetime, it is critically important to measure the driving stresses and the mechanical properties accurately, together with their evolution over time or cycles. It is also necessary to understand the failure mechanisms, which entails careful *ex situ*, *in situ*, and/or *operando* characterization. Furthermore, it is essential to consider coupled effects on the mechanical behavior due to the ubiquitous presence of other stimuli during the operation of perovskite PV, such as environment, light, and electric-field. In this context, comparability of results between different laboratories is important for building consensus regarding tools,

protocols, best practices, and standards. It is imperative that more attention be paid to mechanical reliability of perovskite PV moving forward. A deep understanding of mechanical reliability issues will guide scientific approaches for mitigating them, thereby extending the overall reliability of perovskite PV.

In this Perspective we highlight key challenges and opportunities, together with best practices, pertaining to the three interrelated key elements that determine mechanical reliability: driving stresses, mechanical properties, and mechanical failure. We discuss the sources of driving stresses, along with advantages and disadvantages of the different measurement techniques. We also examine the basic mechanical properties of halide perovskites and interfaces, and their measurements. Furthermore, we review the nature of mechanical failures at the material-, cell-, and module-levels, together with coupled effects. Finally, we discuss characterization approaches for understanding the failure mechanisms, and touch upon the issue of testing standards.

Driving Stresses

Macroscopic, long-range mechanical σ, and derived K or G, in the perovskite thin film that drive failure ('offense') arise from two primary sources. First is equi-biaxial residual tensile stress (σ_R) in the perovskite thin film due to its positive thermal-expansion mismatch ($\Delta\alpha$) with the substrate.[11,17,18] Perovskite films are typically 300-600 nm thin (h_F), while substrates are much thicker (h_S): 1-3 mm glass (E 60-80 GPa) for rigid PV, 100-200 μm plastic (E 3-5 GPa) for flexible PV, and 150-300 μm Si (E~160 GPa) for two-terminal tandem PV. There are other sources of residual stresses, such as those generated during thin-film growth, which are typically more important in vapor-phase deposition and electrodeposition, and in epitaxial growth of single-crystal thin films.[23] Second is externally applied stresses (σ_A), which add to σ_R, as a result of quasi-static loading (*e.g.* stretching, bending, twisting), cyclic loading (*e.g.* wind, vibrations), and/or impact loading (*e.g.* hail, collision). Perovskite thin films also have localized 'microstresses' or 'microstrains' due to the presence of lattice defects, such as vacancies, interstitials, solutes, dislocations, stacking faults.[12,21,22] However, these should not be confused with the long-range σ_R and σ_A that are primarily responsible for mechanical failure discussed here. The accurate quantification of the driving stresses, and their buildup or relaxation over time, poses many challenges, but it also presents plenty of research opportunities. Furthermore, it will help guide strategies, such as tailoring of compositions, microstructures, interfaces, *etc*., for reducing the driving stresses.

Residual Stress. It is challenging to calculate σ_R ($=E_F\Delta\alpha\Delta T/\{1-\nu_F\}$) in perovskite thin films (Fig. 1a) from differential thermal strains because it assumes that the film becomes fully attached to the substrate only at the processing temperature, and that it does not relax during cooling through ΔT to the use temperature. Unfortunately, both these assumptions are likely invalid in many cases. Also, the Young's modulus (E_F) and Poisson's ratio (ν_F) of perovskite thin films of compositions relevant to PV are not known reliably. Furthermore, contributions from other sources for residual stresses are typically not known. Therefore, it is best practice to measure σ_R experimentally.

X-ray diffraction (XRD)- and curvature-based experimental techniques have been used to measure σ_R in perovskite thin films. In XRD, it is best practice to use the self-consistent, eucentric $\sin^2\psi$ method applied to high-index crystallographic planes (Fig. 1b),[24] instead of the artifacts-prone peak-shift measurement only at ψ=0 that is commonly used. However, XRD measures residual strain (ε_R), which needs to be converted to σ_R for mechanical-reliability analyses using

perovskite thin films' E_F and ν_F. Since these elastic properties are not known reliably, all the literature σ_R values are likely unreliable. As better E_F and ν_F measurements of perovskite thin films directly relevant to PV become available, XRD-based σ_R estimates will become more reliable. This also opens up opportunities for developing other analytical techniques that measure ε_R accurately (*e.g.* bulk Raman spectroscopy). This issue is circumvented in curvature-based techniques (*e.g.* multi-optical stress sensor (MOSS) in Fig. 1c) that measure σ_R directly.[23,25] In MOSS, a relatively thin substrate (preferably <0.5 mm) with a highly reflective backside surface is needed for accurate curvature measurements. Using MOSS, σ_R values in the range -11 MPa (compressive) to 58 MPa (tensile) in perovskite thin films have been reported.[17,26] Thus, opportunities exist for innovative adaptation of curvature-based techniques to perovskite thin films.

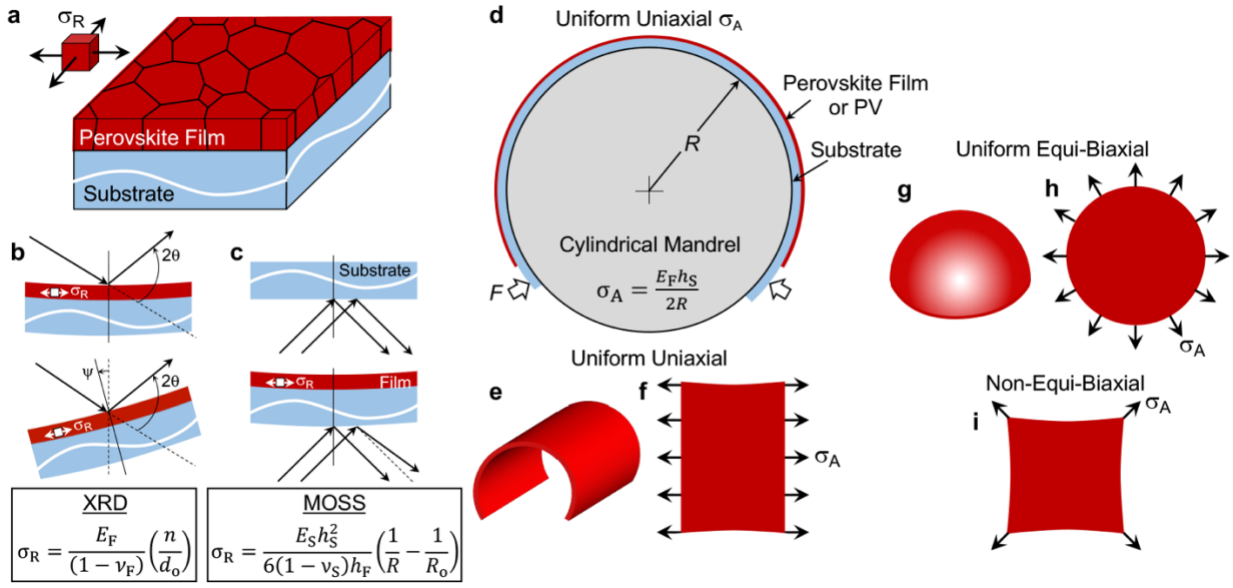

Fig. 1 |Geometry of specimens and set-up configurations for measurement of driving stresses. a, Schematic illustration of polycrystalline perovskite thin film on substrate with equi-biaxial tensile σ_R. **b**, Schematic illustration (cross-section) of the $\sin^2\psi$ XRD method, where d is the interplanar spacing, n is the slope of the d vs. $\sin^2\psi$ data plot, and d_O is the reference interplanar spacing at $\psi = 0$; E_F and ν_F are film Young's modulus and Poisson's ratio, respectively. **c**, Schematic illustration (cross-section) of the MOSS technique, where h_S and h_F are thicknesses of substrate and thin film, respectively; R_O and R are radii-of-curvature before and after thin-film deposition, respectively; and E_S and ν_S are substrate Young's modulus and Poisson's ratio, respectively. Schematic illustrations of cross-section (**d**) and corresponding 3D free-body (**e**) of a perovskite thin film or PV on flexible substrate wrapped around a cylindrical mandrel of radius R to generate uniform uniaxial tensile σ_A (**f**). **g**,**h**, Schematic illustration (3D free-body) of 'dome' bending of a perovskite thin film or PV on flexible substrate wrapped around a sphere of radius R (**g**), to generate uniform equi-biaxial σ_A (**h**). **i**, Schematic illustration of a way to generate non-equi-biaxial σ_A. Not to scale.

Measuring the evolution of σ_R (buildup or relaxation) in buried perovskite thin film within PV as a function of time (constant-temperature testing or thermal-cycling) is a bigger challenge. XRD-based techniques will need high-brightness synchrotrons for probing such thin films, but an intractable challenge is accurate knowledge of the evolving E_F and ν_F with time. In this context, curvature-based techniques are the most promising, and they present exciting opportunities for

their further development to measure the evolution of σ_R, *ex situ* and *operando*.

Applied Stresses. In the case of σ_A, the system-specific loading geometries/conditions can be complex, which often requires finite element analysis (FEA). The simplest situation considered in several studies is bending (convex), using calipers, moveable fixtures, or fingers, of a perovskite thin film, or a PV, on a flexible substrate.[4] However, in this commonly used technique the minimum intended radius-of-curvature (R), and the corresponding maximum σ_A, occurs only at the apex; the rest of the thin film, or the PV, experiences much lower σ_A. This can give misleading results, such as gross underestimation of the degradation across the entire thin film or PV. Thus, it is best practice to wrap the entire thin film or PV around a cylindrical mandrel of radius (R), as shown schematically in Figs. 1d,e to result in uniform uniaxial tensile σ_A (Fig. 1f). In the case of a PV bent this way, the uniaxial ε_A within each of the functional layers is uniform and same (isostrain condition), but the uniform σ_A within each layer is different owing to its different elastic properties of the layers.[20,27,28] The uniaxial tensile σ_A can be estimated analytically using $Eh_S/2R$,[23] where E is the Young's modulus of the layer of interest and h_S is the substrate thickness, which is much thicker than any of the functional layers. Note that such 'cylindrical' convex bending results in Poisson's compressive strain in the perovskite thin film in the width (Fig. 1f) and thickness directions, an important effect that should not be ignored.

For applying equi-biaxial tensile σ_A, the perovskite PV must be bent like a hemispherical 'dome,' as shown schematically in Figs. 1g,h. Alternatively, uniform tensile σ_A can be applied directly, without bending moments, to the thin film, or the PV, attached to flat substrates by stretching them in-plane along: one of the axes to achieve uniaxial σ_A (Fig. 1f), along two orthogonal axes to achieve non-equi-biaxial σ_A (Fig. 1i), or equally in all directions to achieve equi-biaxial σ_A (Fig 1h).[29,30] This requires effective methods for attaching the substrate edges to the loading device, which can be a challenge. Once again, the accuracy of σ_A and its spatial distribution calculated using analytical and FEA modeling is only as good as the accuracy of E_F and ν_F of the perovskite thin film (and corresponding E and ν of the other functional layers in the PV), and their evolution over time, which is discussed next.

Mechanical Properties

The primary basic mechanical properties of halide perovskites that offer 'defense' against the above stresses include: stiffness (E), resistance to elastic deformation; hardness (H), resistance to plastic (localized) deformation; and toughness (K_{IC} or G_C), resistance to crack propagation. Some of these properties are expected to decay over time as damage accumulates. Also at play are inherently time-dependent mechanical damage processes, such as creep and fatigue. Furthermore, the presence of other stimuli such as environment, light, and electric-field, which are ubiquitous during the operation of perovskite PV, can influence the mechanical behavior (*i.e.* coupled effect), beyond the obvious effects from wholesale chemical degradation of the perovskite materials and interfaces. Once again, the accurate quantification of these properties of halide perovskites relevant to PV, and their evolution over time, poses numerous challenges, but it also presents vast research opportunities.

Elasticity. There are some reports of indirect E measurements using nanoindentation, and full stiffness matrix (C_{ij}) measurements using spectroscopies.[12] However, there are only two studies that directly measure E of halide perovskites (ν has not yet been measured directly). Ahn, *et al*.[31] report E ~5.5 GPa and ~4.5 GPa for $MAPbI_3$ and $MAPb(I_{0.87}Br_{0.13})_3$, respectively, for free-standing

polycrystalline thin films tested in uniaxial tension (Fig. 2a). For bulk single-crystals, Dai, *et al*.[13] report $E_{<100>}$ of 10.6±1.0 GPa and 13.1±1.3 GPa for $MAPbI_3$ and $MAPbBr_3$, respectively, tested in uniaxial compression, where the ~25% higher E of $MAPbBr_3$ is attributed to the shorter and stronger Pb-Br bonds in the $PbBr_6^{4-}$ octahedra 3D network that controls the stiffness of halide perovskites. (Note that E of $MAPbI_3$ single-crystals measured using nanoindentation ranges from 10.4 to 23.92 GPa. Tu, 2021 #4219] This wide range can be attributed to the fact that nanoindentation is an indirect, surface-sensitive method, and the results critically depend on the surface conditions and the testing parameters.) Most recently, E of 6.1-6.2 GPa is reported for polycrystalline $MAPbI_3$ thin films attached to substrates using a new indirect method: combination of XRD $\sin^2\psi$ and MOSS techniques.[32] Almost a factor of two reduction in the E of $MAPbI_3$ polycrystalline thin films measured in tension speaks to the possible effects of grain boundaries, pre-existing cracks, *etc*., which are not fully understood at this time. The main elastic-properties measurement challenge is the small size of specimens which are not amenable to conventional standardized mechanical testing.

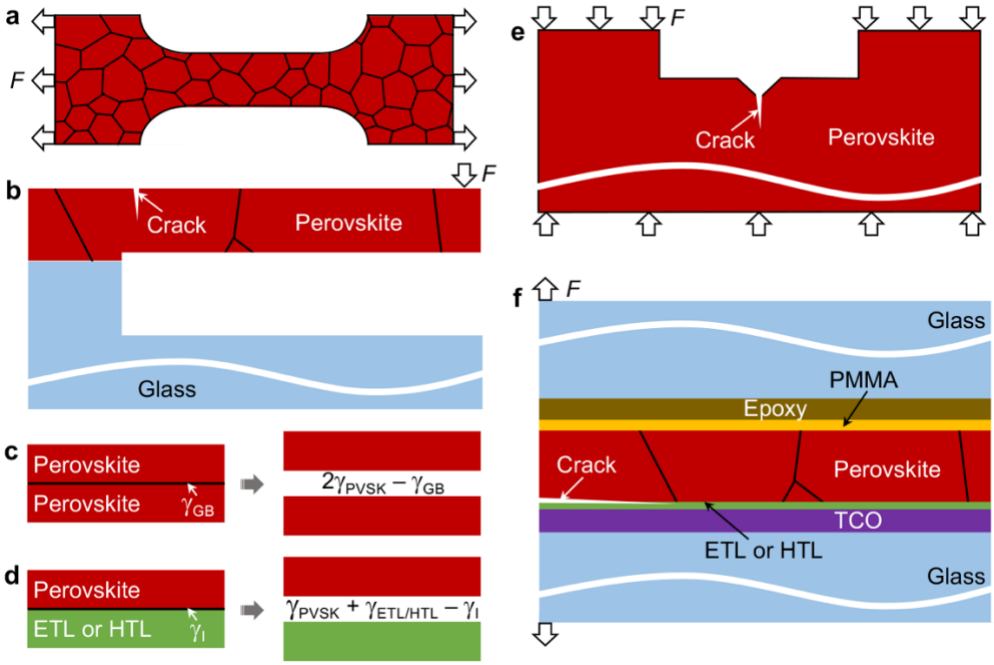

Fig. 2 | Geometry of specimens and set-up configurations for the measurements of mechanical properties. a, Schematic illustration (top view) of uniaxial tensile micro-testing of 'dog bone' specimen of a polycrystalline free-standing thin film for E measurement (F is applied force). **b**, Schematic illustration (cross-section) of microcantilever beam bending for K_{IC} measurement (with the crack) and E measurement (without the crack). Schematic illustrations of grain-boundary (**c**) and interfacial fracture (**d**), and the corresponding energy-balance concepts. **e**, Schematic illustration of the double-cantilever in compression micro-testing geometry for K_{IC} measurement. f, Schematic illustration of the DCB geometry for interfacial G_C measurement. Not to scale.

Uniaxial tensile micro-testing of 'dog bone' specimens (microns long) machined out of free-standing perovskite thin films (sub-micron thickness) using focused ion beam (FIB) is the most direct technique (Fig. 2a).[31] However, this requires complicated micro-electromechanical system (MEMS) devices,[31,33] and unlike in PV, the thin films are not attached to substrates. Another approach is to FIB-out microcantilevers from thin films and perform micro-bend-testing

(Fig. 2b),[34] which is yet to be applied to halide perovskites. However, in both techniques the issue of FIB-induced damage of the beam-sensitive perovskite thin films must be resolved, *e.g.* by using low-dose methods. This shortcoming is alleviated in cm-sized single-crystal perovskite specimens that can be mechanically machined, but results from such specimens are more relevant for basic mechanical behavior studies, and once again, would represent upper bounds. Thus, ample opportunities exist for directly measuring E and ν of halide perovskites in a form most relevant to PV, *i.e.* polycrystalline thin films attached to substrates, using innovative micro-testing, and understanding the effects of grain boundaries, microstructure, cracks, composition, anisotropy, specimen size, *etc*. The microcantilever-based techniques could also be used to quantify the evolution of the elastic properties of perovskite thin films over time as damage accumulates.

Plasticity. H quantifies the resistance to plastic deformation (localized under the intense pressure of a sharp diamond indenter) of highly brittle materials like halide perovskites that do not show yielding in uniaxial tensile tests.[31] Vickers micro-hardness is reliable for bulk materials as it samples larger depth/area and minimizes the undesirable indentation-size effects common among nanoindentation.[35] For example, the Vickers technique was recently used to measure accurate H values of $MAPbI_3$ and $MAPbBr_3$ bulk single-crystals to be 0.76±0.05 GPa and 0.54±0.02 GPa, respectively.[13] However, in the case of perovskite thin films, there is no alternative to nanoindentation and low loads. While this minimizes substrate effects by maintaining indentation-depth <10% film-thickness, it is surface-sensitive and also results in artificially high H values due to the 'indentation-size effect.'[35] This presents a challenge for accurate quantification of H, but offers opportunities for innovations in H measurements, with implications beyond perovskite thin films.

It appears that dislocation plasticity controls H, which explains the higher H of $MAPbI_3$ with lower crystal symmetry compared to $MAPbBr_3$, but detailed mechanisms of plastic deformation (prevalent slip systems) in halide perovskites,[36] and their possible effects on the optoelectronic properties, are unknown. Also, creep deformation of halide perovskites, *i.e.* time-dependent permanent deformation under constant load at room temperature, invariably involves ion-migration, by itself or in conjunction with dislocation plasticity, but very little is known about the mechanisms.[13,36] Thus, there are ample opportunities for basic studies in these areas, with profound implications for perovskite PVs' mechanical reliability.

Fracture. Fracture of highly brittle halide perovskites, driven by K or G at the crack tip arising from σ_R and/or σ_A, is resisted solely by their fracture toughness, K_{IC} (tensile opening mode I) or G_C. (Fracture strength (σ_F) of brittle materials such as halide perovskites is not an inherent material property as it critically depends on the geometry and size of the largest crack (c^*) present in the material.[37]) K_{IC} is an inherent mechanical property, and is given by $Y\sigma_F(c^*)^{0.5}$, where Y is crack-geometry parameter. Toughness can also be expressed in terms of energy, G_C (cohesion) $=K_{IC}^2/E'$, where $E'=E/(1-\nu^2)$ (plane strain, thick bulk) or $E'=E$ (plane stress, thin plate).[37] Here G_C identifies with $2\gamma_{PVSK}$, where γ_{PVSK} is the surface energy of the halide perovskite. Recently, the K_{IC} values of $MAPbI_3$ and $MAPbBr_3$ single-crystals have been measured, using the Vickers micro-indentation technique,[37] to be 0.18±0.03 $MPa.m^{0.5}$ and 0.20±0.03 $MPa.m^{0.5}$, respectively,[13] which translate to G_C of ~3 $J.m^{-2}$ (plane stress) for both. These represent upper bounds, because experimentally measured grain-boundary toughness is found to be significantly lower; *e.g.* some polycrystalline $MAPbI_3$ thin films have G_C as low as 0.41±0.17 $J.m^{-2}$ (K_{IC}~0.06 $MPa.m^{0.5}$).[38] Here G_C identifies with $(2\gamma_{PVSK} - \gamma_{GB})$, where γ_{GB} is the grain-boundary energy. In the case of interfaces between halide perovskite and dissimilar materials, *e.g.* perovskite/ETL (electron transport layer) or

perovskite/HTL (hole transport layer), in the PV, the interfacial toughness is always expressed in terms of G_C (adhesion), which identifies with ($\gamma_{PVSK} + \gamma_{ETL} - \gamma_I$) or ($\gamma_{PVSK} + \gamma_{HTL} - \gamma_I$), where γ_{ETL} or γ_{HTL} is the ETL or HTL surface energy, respectively, and γ_I is the corresponding interface energy. These energy-balance concepts are depicted schematically in Figs 2c,d. Thus, counterintuitively, γ_{GB} and γ_I must be reduced to improve grain-boundary and interfacial toughness, respectively. Overall, the critical condition for fast fracture is $K \geq K_{IC}$ or $G \geq G_C$, where the driving K or G depend on both the driving stresses (σ_R and/or σ_A), and the crack size/geometry.[37]

All the K_{IC} measurements of halide perovskites are using indentation techniques on bulk single-crystals, but these are indirect methods. Thus, there are opportunities to measure K_{IC} of bulk halide perovskites directly using established fracture-mechanics testing of cm-sized samples (Fig. 2e),[39] and of thin films using emerging small-volume testing techniques (Fig. 2b);[33,40] both are yet to be applied to halide perovskites. Cohesion G_C of halide perovskites and adhesion G_C of different interfaces relevant to PV, have been measured using the double-cantilever-beam (DCB) technique, which is a proper fracture-mechanics test, but it is somewhat involved (Fig 2f). In this context, it may be tempting to use the simpler 'direct-pull' or 'scotch-tape peel' tests to assess adhesion toughness. However, these semi-quantitative tests are likely to give misleading results, because the critically important parameters of crack geometry and size are not considered. There are also opportunities for expanding the DCB test for testing full perovskite PV at scale, instead of the current primarily isolated 'model' interfaces or partial-cells, which is likely to provide valuable information about the mechanical properties at the cell and module levels. Furthermore, DCB testing can be extended for studying cyclic-fatigue effects on the fracture of halide perovskites and interfaces, and also coupled effects.

Mechanical Failure

Understanding mechanical failure is as important as the above quantification of driving stresses and mechanical properties, and it is key to designing scientifically sound approaches for failure mitigation. Mechanical failures can occur at the following three hierarchical levels. First, at the material-level, failure refers to fracture (loss of mechanical integrity) of the perovskite thin film or the interface in question. Second, at the cell-level, failure refers to specified loss in the PV performance primarily due to the loss of mechanical integrity. Third, at the module-level, failure refers to loss of mechanical integrity of the additional layers and/or interfaces. Despite the critical importance of mechanical failure in determining mechanical reliability, published research in this area is the least developed, and in the case of modules it is non-existent. The challenges associated with understanding and mitigating mechanical failures at these levels are formidable, but there are unprecedented opportunities to overcome them.

Material Failure. Fracture within the perovskite thin film and/or at the interfaces is the most consequential form of mechanical failure in perovskite PV.[19,20] Fracture in perovskite thin films typically initiates from incipient flaws (grain-boundary grooves, pre-existing cracks), or from damage generated during operation (voids, plastic deformation, creep, material degradation), and is driven by K or G. The simplest case is the through-thickness propagation of an incipient surface crack ($2c^*$ diameter) into (z direction) the perovskite thin film (Figs. 3a,d).[11] The crack will subsequently 'channel' across (x direction) the width of the thin film (Figs. 3b,e).[11] This staggered sequence of cracking typically occurs at multiple locations simultaneously, resulting in arrays of parallel 'channel' cracks with increasing stresses and/or fatigue effects. Since these cracks are

narrow and 'vertical,' they may not affect the photocarriers transport across the perovskite thin film significantly if confined to that layer; the loss in the active area due to saturated arrays of such cracks is expected to be <2%. However, these 'invisible' cracks may result in faster environmental degradation of the halide perovskites and interfaces due to more facile ingression of the environmental species (coupled effects), which have not been adequately considered in some prior studies. The most serious impact of these 'vertical' cracks is that they provide a plethora of internal free surfaces which are necessary for the initiation and growth of the more dangerous 'horizontal' (in *x*-*y* plane) interfacial cracks (delamination) (Fig. 3c).[11] Such interfacial cracks can also initiate from voids generated at the interfaces during perovskite PV operation (see *e.g.* Figs. 3f,g). Examples of channel cracks, and associated interfacial cracks, are shown in Figs. 3h,i. Figure 3j summarizes schematically the possible evolution of cracking in a perovskite PV during operation.

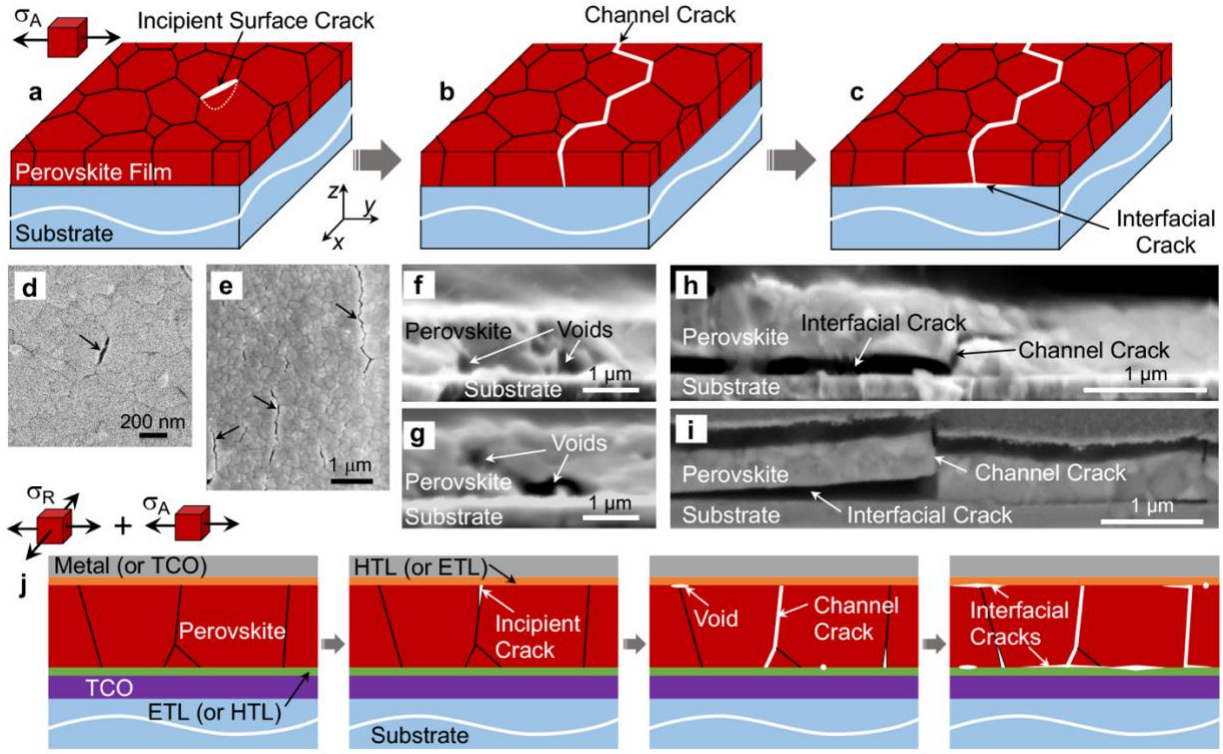

Fig. 3 | Types of mechanical failures at material and device levels. a,**b**,**c**, Schematic illustration of sequence of cracking in a perovskite thin film subjected to σ_A. SEM images (top view) showing examples of initial surface crack (**d**) and channel crack (**e**) in a $MAPbI_3$ perovskite thin film. **f-i**, SEM images (cross-section) of a rigid PSC tested for 757 h under continuous 1-sun illumination under maximum-power-point tracking (**f-h**) and a flexible perovskite PV tested in cyclic bending (R=5 mm) for 10,000 cycles (**i**), showing examples of voids, channel cracks and interfacial cracks. **j**, Schematic illustration (cross-section) of possible evolution of cracking in perovskite PV during operation under a combination of σ_R and σ_A. Schematic illustrations not to scale. Figures adapted with permission: **a**,**b**,**c**,**i**, ref.[20] from Wiley; **d**, ref.[54] from Elsevier; **e**, ref.[27] from Elsevier; **f,g,h**, ref.[19] from AAAS.

The main challenges in understanding failure mechanisms are specimen preparation and characterization of the exact nature of the cracks. For example, care must be taken in obtaining cross-sections of perovskite PV (*e.g.* Figs. 3h-i) to avoid introducing additional cracking during specimen preparation. Also, narrow cracks, where the crack-walls are in contact, are typically

'invisible.'[27] In this context, the only true test of presence or absence of crack is inability or ability, respectively, of the perovskite thin film to sustain tensile stresses.[27] Regarding observing cracks in the scanning electron microscope (SEM), the very act can result in cracking, obscuring preexisting cracks.[27] Thus, low-dose SEM techniques need to be developed. Also, there are opportunities to develop entirely new techniques that utilize acoustic, thermal, or optical probes for the detection and characterization/imaging of cracks in perovskite thin films and at interfaces, and their evolution with time.

Comprehensive understanding of failure of halide perovskites and interfaces, together with tools/protocols for accurate mechanical properties measurements, provides many opportunities to reduce and/or delay fracture, thereby enhancing the mechanical reliability of perovskite PV. For example, the 'vertical' cracking of halide perovskites, which is a precursor to subsequent 'channel' and interfacial cracking, can be delayed by reinforcing the surface cracks by low-dimensional (LD) halide perovskite 'sealing' layer (*i.e*. effectively strengthening the 3D halide perovskite thin film) for extending cyclic fatigue life of flexible PV.[20,28] Also, there are opportunities to toughen the perovskite grain boundaries themselves. Furthermore, facile crack-healing properties unique to halide perovskites could be exploited to reverse material failure.[27]

Regarding interfaces, those between perovskite and ETL or HTL, can be rationally tailored to increase the interfacial toughness for improved PV durability. For example, by incorporating a molecular layer,[41] a cross-linkable fullerene layer,[42] a polymer layer,[43], a self-assembled monolayer,[19] or a LD perovskite,[20] at either the perovskite/HTL or the perovskite/ETL interface, significant improvements in the interfacial G_C have been achieved, and are now approaching the upper bound G_C of single-crystal halide perovskites (~3 $J.m^{-2}$).[19] Also, the mechanical robustness imparted by such strengthening/toughening of perovskite thin films and interfaces will be beneficial for down-stream modules manufacturing processes such as scribing, encapsulation, lamination, *etc*. Many more new failure-mitigation approaches await invention, but they will be successful in the long run only if they are based on sound mechanics-of-materials principles and proper testing. Of course, any of these strengthening/toughening approaches must lead to either no deficit, or simultaneous enhancement, in the PV performance.[19,20]

<u>*Coupled Effects.*</u> The coupled effects of environment, light, and electric-field on the mechanical behavior of halide perovskites and interfaces as they pertain to mechanical reliability have not been studied in any detail (Fig. 4a). There are scattered reports of coupled properties such a ferroelasticity,[44] ferroelectricity,[45] piezoelectricity,[46] photo-ferroelasticity,[47] and photostriction [48] in halide perovskites, but they are not in the context of mechanical reliability. Regarding environment, even dilute species (H_2O, O_2, gaseous reaction products, *etc*.) are likely to influence fracture of halide perovskites and interfaces, where they can attack the chemical bonds at the crack tip, and concomitantly decrease the surface energies substantially (Fig 4b). The net result is slow crack-growth that can occur under constant stress at sub-critical conditions (so-called static-fatigue), $K \leq K_{IC}$ or $G \leq G_C$,[37] which will add time-dependence to the failure. Under cyclic loading, the crack can also propagate slowly at lower net $K \leq K_{IC}$ or $G \leq G_C$,[37] *i.e.* cyclic-fatigue effect, which makes the failure of materials and interfaces cycle-dependent (Fig. 4c). Regarding light, it may affect plasticity (H) (Fig. 4d) and creep (Fig. 4e) deformation in halide perovskites *via* photocarriers-mediated effects on dislocations dynamics, which needs to be explored. It is not clear if light will affect K_{IC} or G_C of halide perovskites and interfaces, but electric-field may influence them *via* possible ion-migration-mediated charging. Similarly, electric-field may affect creep deformation (Fig. 4e) *via* facile ion-migration prevalent in halide perovskites. Thus, there are

ample opportunities to study such coupled effects due to a combination of these stimuli, which are likely to have a direct bearing on the mechanical reliability of perovskite PV.

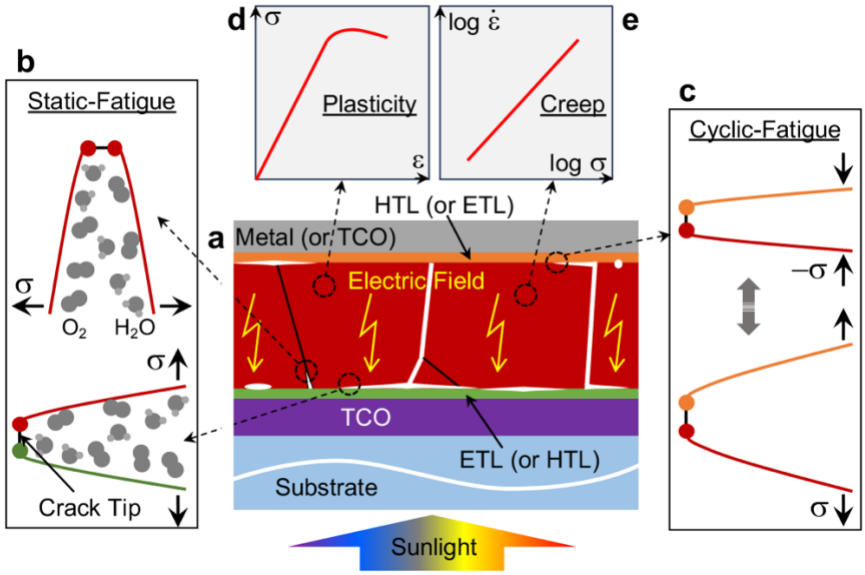

Fig. 4 | Coupled effects of environment, light, and electric field on deformation and fracture. Schematic illustrations (cross-section) of possible coupled effects in halide perovskites and interfaces (**a**): static-fatigue (**b**), cyclic-fatigue (**c**), plasticity (**d**), and creep (**e**). Strained atomic bonds at the crack tip depicted schematically in (**b**) and (**c**) for fracture within perovskite (top in (**b**)) and at interfaces (bottom in (**b**), (**c**)). Colors of the atoms (spheres) and the crack walls (curves) correspond to the colors of the materials in (**a**). Not to scale.

Cell Failure. Since specified loss in performance of a perovskite PV can be due to myriad reasons, identification of that specifically due to mechanical failure is a difficult task. Here, *postmortem* characterization of operated PV, together with the partial-cell mechanical testing, can yield valuable insights into the role of mechanical failure in the decay of performance; *e.g.* mechanical damage is seen in the cross-sectional SEM image Figs. 3f,g,h of a rigid PV operated for 757 hours.[19] Flexible PV are amenable to full-cell mechanical testing, in static and cyclic bending around a cylindrical mandrel (Figs. 1d,e), where in the latter, in addition to the peak σ_A induced in the different layers of the PV, the bending-cycling parameters and conditions are important.[20,28] For example, the flat→convex→flat 'half' cycle is recommended to understand cyclic-fatigue effects,[20,28] instead of the typically used flat→convex→flat→concave→flat 'full' cycle,[4] to preclude any indeterminate crack-healing effects during the concave (compression) part of the cycle.[27] This, in conjunction with *postmortem* characterization, provides valuable information about their mechanical reliability; *e.g.* the cross-sectional SEM image in Fig. 3i of a flexible PV tested for 10,000 bending cycles shows performance degradation due to mechanical damage.[20] Once again, the challenge is the preservation of the mechanical-damage features during specimen preparation such as cross-sectioning. This presents opportunities for the development of new methods for specimen preparation and/or high-resolution characterization of buried mechanical failures in PV non-destructively, where the latter could be implemented *operando*. Also, there are opportunities for further development and automation of partial- and full-cell mechanical testing.

Module Failure. The development of perovskite modules is in its infancy,[49,50] and there is great

uncertainty regarding architectures, materials, assembly, and manufacturing. Not much is known about their mechanical failure, with the possible exception of a small study on encapsulated perovskite PV.[51] This presents a unique opportunity to incorporate mechanical-reliability considerations in the initial design of perovskite modules and their manufacturing. This could include consideration of mechanical properties in materials selection, and strategies to achieve high adhesion G_C and reduced driving stresses for mitigating the formation of interfacial cracks and 'blistering' (Fig. 5). For example, higher interfacial G_C will reduce the propensity for interfacial cracking induced by laser-scribing used in the manufacturing of perovskite modules and tandem PV (Fig. 5). Similar interfacial toughening approaches could be used in the cases of encapsulants and backsheets. In this context, the single-cantilever beam technique developed for Si-based modules [52] could be used for measuring the adhesion G_C between module layers. Also, lower-E encapsulants and backsheets can result in lower driving stresses. Furthermore, *postmortem* characterization can provide useful insights into the failure mechanisms at the module-level, where established tools and procedures used for Si-based PV could be adapted.

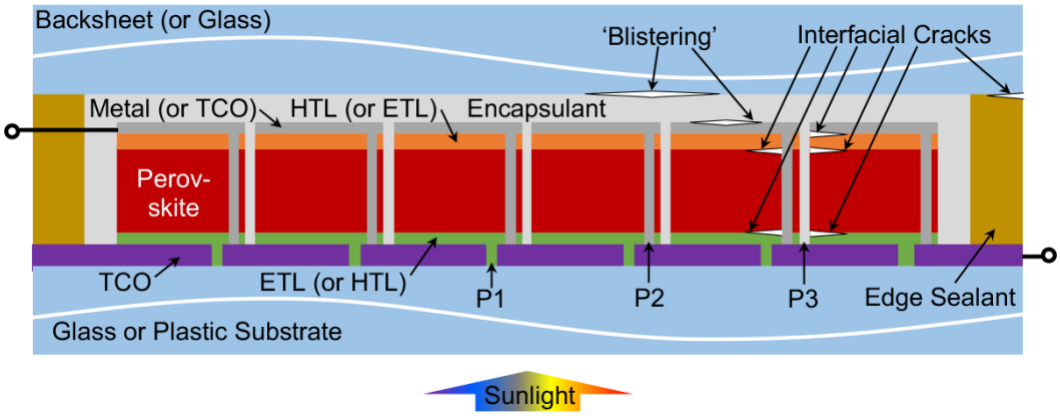

Fig. 5 | Module failure modes. Schematic illustration (cross-section) of examples of interfacial cracking and blistering in a typical perovskite mini-module architecture for regular, bifacial, or four-terminal tandem PV (P1, P2, and P3 are successively scribed channels). Not to scale.

Regarding existing module-testing standards, IEC 61215 is widely used for the minimum requirements ('pass-fail') of commercial Si-based PV.[53] Within IEC 61215 there are five tests that pertain to mechanical behavior of modules: thermal-cycling (MQT 11), static-mechanical loading (MQT 16), hail (MQT 17), dynamical-mechanical loading (MQT 20), and bending (only for flexible modules) around a cylindrical mandrel (MQT 22). However, IEC 61215 standard sets the minimum short and long dimension of the module at 0.75 m and 1.1 m, respectively; perovskite modules of this minimum size do not exist. Importantly, due to the very nature of some of the specified tests they cannot be simply scaled down to perovskite module sizes. Thus, with the possible exception of MQT 11, the IEC 61215 standard cannot be applied directly to current perovskite modules. This presents opportunities for developing new 'pass-fail' mechanical tests pertinent to perovskite modules for inclusion in future standards, informed by the above mechanical-reliability studies. For example, MQT 16 is based on cantilever deflection, where a minimum of 2.4 KPa dead-weight load spread over a center-supported 0.7×1.1 m^2 module; here the absolute size and the elastic properties of the materials are critically important. Thus, MQT 16 will need to be modified such that it is valid for the size and elastic properties of the future commercial perovskite modules. In the case of two-terminal tandem modules (perovskite on Si)

the changes needed for the current IEC 61215 mechanical tests may be minimal, provided future commercial tandem modules meet the minimum size requirement.

Finally, the strong interrelationships between the three key elements — driving stresses, mechanical properties, mechanical failure — discussed in the context of the mechanical reliability of materials, cells, and modules cannot be overemphasized. For example, accurate measurement of driving stresses are strongly dependent on the accurate knowledge of the elastic properties of the materials. Also, accurate measurements of both the driving stresses and the mechanical properties are needed to determine the failure of perovskites thin films and interfaces. Furthermore, characterization and understanding of the failure mechanisms and coupled effects can inform mitigation strategies, but accurate measurements are needed to ascertain driving stresses reduction and/or mechanical properties improvements. This underscores the importance of integrated studies of the three key elements in addressing mechanical reliability of perovskite PV.

Conclusions

Mechanical reliability issues need to be addressed before perovskite PV can be field-deployed successfully — increased awareness of its importance and a concerted, integrated research effort will go a long way in making this possible. There is an urgent need for developing tools and protocols for accurate quantification of driving stresses and mechanical properties, with an eye towards understanding failure modes/mechanisms and coupled effects at the material, cell, and module levels. Also, it is important to have comparability of results between laboratories, and to build community consensus regarding best practices, through round-robin studies and consensus statements, respectively. Taking advantage of the opportunities highlighted in this Perspective by the community as a whole to overcome the outlined challenges will contribute towards meaningful progress in addressing the unproven reliability of this promising new thin-film PV technology.

References

1 Miyasaka, T. *Perovskite Photovoltaics and Optoelectronics: From Fundamentals to Advanced Applications*. (Wiley-VCH, 2021).

2 Luo, X. *et al.* Recent progress in perovskite solar cells: from device to commercialization. *Sci. China Chem.* **65**, 2369-2416 (2022).

3 Padture, N. P. The promise of metal-halide-perovskite solar photovoltaics: A brief review. *MRS Bull.* in press (2023). (DOI:10.1557/s43577-023-00585-6)

4 Gao, Y. *et al.* Flexible perovskite solar cells: From materials and device architectures to applications. *ACS Energy Lett.* **7**, 1412-1445 (2022).

5 Koh, T. M. *et al.* Halide perovskite solar cells for building integrated photovoltaics: Transforming building façades into power generators. *Adv. Mater.* **34**, 2104661 (2022).

6 Delmas, W. *et al.* Evaluation of hybrid perovskite prototypes after 10-month space flight on the international space station. *Adv. Energy Mater.* **13**, 2203920 (2023).

7 Fu, W. *et al.* Stability of perovskite materials and devices. *Mater. Today* **58**, 275-296 (2022).

8 Dunfield, S. P. *et al.* From defects to degradation: A mechanistic understanding of degradation in perovskite solar cell devices and modules. *Adv. Energy Mater.* **10**, 1904054 (2020).

9 Siegler, T. D. *et al.* The path to perovskite commercialization: A perspective from the United States Solar Energy Technologies Office. *ACS Energy Lett.* **7**, 1728-1734 (2022).

10 Rolston, N. *et al.* Mechanical integrity of solution-processed perovskite solar cells. *Extreme Mech. Lett.* **9**, 353-358. (2016).
11 Ramirez, C., Yadavalli, S. K., Garces, H. F., Zhou, Y. & Padture, N. P. Thermo-mechanical behavior of organic-inorganic halide perovskites for solar cells. *Scripta Mater.* **150**, 36-41 (2018).
12 Tu, Q., Kim, D., Shyikh, M. & Kanatzidis, M. G. Mechanics-coupled stability of metal-halide perovskites. *Matter* **4**, 2765-2809 (2021).
13 Dai, Z. *et al.* The mechanical behavior of metal-halide perovskites: Elasticity, plasticity, fracture, and creep. *Scripta Mater.* **223**, 115064 (2023).
14 Hopcroft, M. A., Nix, W. D. & Kenny, T. W. What is the Young's modulus of silicon? *J. MEMS.* **19**, 229-238 (2010).
15 Berriche, R. Vickers hardness from plastic energy. *Scripta Mater.* **32**, 617-620 (1995).
16 Sebastiani, M., Johanns, K. E., Herbert, E. G. & Pharr, G. M. Measurement of fracture toughness by nanoindentation methods: Recent advances and future challenges. *Curr. Opin. Solid State Mater. Sci.* **19**, 324-333 (2015).
17 Rolston, N. *et al.* Engineering stress in perovskite solar cells to improve stability. *Adv. Energy Mater.* **8**, 1802139 (2018).
18 Dailey, M., Li, Y. & Printz, A. D. Residual film stresses in perovskite solar cells: Origins, effects, and mitigation strategies. *ACS Omega* **6**, 30214-30223 (2021).
19 Dai, Z. *et al.* Interfacial toughening with self-assembled monolayers enhances perovskite solar cells reliability. *Science* **372**, 618-622 (2021).
20 Dai, Z. *et al.* Dual-interface reinforced flexible perovskite solar cells for enhanced performance and mechanical reliability. *Advanced Mater.* **34**, 2205301 (2022).
21 Liu, D. *et al.* Strain analysis and engineering in halide perovskite photovoltaics. *Nature Mater.* **20**, 1337-1346 (2021).
22 Yang, B. *et al.* Strain effects on halide perovskite solar cells. *Chem. Soc. Rev.* **51**, 7509-7530 (2022).
23 Freund, L. B. & Suresh, S. *Thin Film Materials: Stress, Defect Formation and Surface Evolution*. (Cambridge University Press, 2003).
24 Luo, Q. & Jones, A. H. High-precision determination of residual stress of polycrystalline coatings using optimised XRD-sin$^2\psi$ technique. *Surf. Coat. Technol.* **205**, 1403-1408 (2010).
25 Chason, E. & Guduru, P. R. Tutorial: Understanding residual stress in polycrystalline thin films through real-time measurements and physical models. *J. Appl. Phys.* **119**, 191101 (2016).
26 Hovish, M. Q. *et al.* Crystallization kinetics of rapid spray plasma processed multiple cation perovskites in open air. *J. Mater. Chem. A* **8**, 169-176 (2020).
27 Yadavalli, S. K., Dai, Z., Zhou, H., Zhou, Y. & Padture, N. P. Facile crack-healing in organic-inorganic halide perovskite thin films. *Acta Mater.* **187**, 112-121 (2020).
28 Dong, Q. *et al.* Flexible perovskite solar cells with simultaneously improved efficiency, operational stability, and mechanical reliability. *Joule* **5**, 1587-1601 (2021).
29 Kaltenbrunner, M. *et al.* Flexible high power-per-weight perovskite solar cells with chromium oxide–metal contacts for improved stability in air. *Nature Mater.* **14**, 1032-1041 (2015).
30 Dauzon, E. *et al.* Pushing the limits of flexibility and stretchability of solar cells: A review. *Advanced Mater.* **33**, 2101469 (2021).

31 Ahn, S.-M. *et al.* Nanomechanical approach for flexibility of organic-inorganic hybrid perovskite solar cells. *Nano Lett.* **19**, 3707-3715 (2019).

32 Layek, M. *et al.* Elastic modulus of polycrystalline halide perovskite thin films on substrates. *http://arxiv.org/abs/2307.07071* (2023). (Accessed September 10, 2023)

33 Dehm, G., Jaya, B. N., Raghavan, R. & Kirchlechner, C. Overview on micro- and nanomechanical testing: New insights in interface plasticity and fracture at small length scales. *Acta Mater.* **142**, 248-282 (2018).

34 Armstrong, D. E. J., Wilkinson, A. J. & Roberts, S. G. Measuring anisotropy in Young's modulus of copper using microcantilever testing. *J. Mater. Res.* **24**, 3268-3276 (2009).

35 Fischer-Cripps, A. C. Critical review of analysis and interpretation of nanoindentation test data. *Surf. Coat. Technol.* **200**, 4153-4165 (2006).

36 Reyes-Martinez, M. A. *et al.* Time-dependent mechanical response of $APbX_3$ (A=Cs, CH_3NH_3; X=I, Br) Single Crystals. *Adv. Mater.* **29**, 1606556 (2017).

37 Lawn, B. R. *Fracture of Brittle Solids — Second Edition*. (Cambridge University Press, 1993).

38 Dai, Z. *et al.* Effect of grain size on the fracture behavior of organic-inorganic halide perovskite thin films for solar cells. *Scripta Mater.* **185**, 47-50 (2020).

39 Wang, Q. *et al.* Fracture, fatigue, and sliding-wear behavior of nanocomposites of alumina and reduced graphene-oxide. *Acta Mater.* **186**, 29-39 (2020).

40 Ast, J. *et al.* A review of experimental approaches to fracture toughness evaluation at the micro-scale. *Mater. Desig.* **173**, 107762 (2019).

41 Yun, J. H. *et al.* Synergistic enhancement and mechanism study of mechanical and moisture stability of perovskite solar cells introducing polyethylene-imine into the $CH_3NH_3PbI_3$/HTM interface. *J. Mater. Chem. A* **3**, 2176-2182 (2015).

42 Watson, B. L. *et al.* Cross-linkable, solvent-resistant fullerene contacts for robust and efficient perovskite solar cells with increased J_{SC} and V_{OC}. *ACS Appl. Mater. Interf.* **8**, 25896-25904 (2016).

43 Jeong, S., Lee, I., Kim, T.-S. & Lee, J.-Y. An interlocking fibrillar polymer layer for mechanical stability of perovskite solar cells. *Adv. Mater. Interf.* **7**, 20001425 (2020).

44 Kutes, Y. *et al.* Direct observation of ferroelectrtic domains in solution-processed $CH_3NH_3PbI_3$ perovskite thin films. *J. Phys. Chem. Lett.* **5**, 3335-3339 (2014).

45 Strelcov, E. *et al.* $CH_3NH_3PbI_3$ Perovskites: Ferroelasticity revealed. *Sci. Adv.* **3**, e1602165 (2017).

46 Kim, D. B., Park, K. H. & Cho, Y. S. Origin of high piezoelectricity of inorganic halide perovskite thin films and their electromechanical energy-harvesting and physiological current-sensing characteristics. *Energy Environ. Sci.* **13**, 2077-2086 (2020).

47 Liu, Y. *et al.* Light-ferroic interaction in hybrid organic-inorganic perovskites. *Adv. Opt. Mater.* **7**, 1901451 (2019).

48 Zhou, Y. *et al.* Giant photostriction in organic-inorganic lead halide perovskites. *Nature Commun.* **7**, 11193 (2016).

49 Kim, D. H., Whitaker, J. B., Li, Z., Hest, M. F. A. M. v. & Zhu, K. Outlook and challenges of perovskite solar cells toward terawatt-scale photovoltaic module technology. *Joule* **2**, 1437-1451 (2018).

50 Pescetelli, S. *et al.* Integration of two-dimensional materials-based perovskite solar panels into a stand-alone solar farm. *Nature Energy* **7**, 597-607 (2022).

51 Cheacharoen, R. *et al.* Design and understanding of encapsulated perovskite solar cells to withstand temperature cycling. *Energy Environ. Sci.* **11**, 144-150 (2018).
52 Novoa, F. D., Miller, D. C. & Dauskardt, R. H. Environmental mechanisms of debonding in photovoltaic backsheets. *Solar Energy Mater. Solar Cells A* **120**, 87-93 (2014).
53 IEC61215-1:2021. in *https://webstore.iec.ch/publication/61345* (Ed Technical Committee 82) (IEC, 2021). (Accessed on September 10, 2023)
54 Yadavalli, S. K., Hu, M., Dai, Z., Zhou, Y. & Padture, N. P. Electron-beam-induced cracking in organic-inorganic halide perovskite thin films. *Scripta Mater.* **187**, 88-92 (2020).

Acknowledgements

We are grateful for the funding from Office of Naval Research (Grant No. N00014-20-1-2574), National Science Foundation (Grant No. DMR-2102210), and Department of Energy (DOE) Office of Energy Efficiency and Renewable Energy under the Solar Energy Technology Office (Award No. DE-0009511). The views expressed in the article do not necessarily represent the views of DOE or the U.S. Government.

Competing interests

The authors declare no competing interests.

Additional information

Correspondence should be addressed to Nitin P. Padture.